

Giant leaps and long excursions: fluctuation mechanisms in systems with long-range memory

Robert L. Jack^{1,2} and Rosemary J. Harris³

¹*Department of Applied Mathematics and Theoretical Physics,
University of Cambridge, Wilberforce Road, Cambridge CB3 0WA, United Kingdom*

²*Department of Chemistry, University of Cambridge,
Lensfield Road, Cambridge CB2 1EW, United Kingdom*

³*School of Mathematical Sciences, Queen Mary University of London,
Mile End Road, London E1 4NS, United Kingdom*

We analyse large deviations of time-averaged quantities in stochastic processes with long-range memory, where the dynamics at time t depends itself on the value q_t of the time-averaged quantity. First we consider the elephant random walk and a Gaussian variant of this model, identifying two mechanisms for unusual fluctuation behaviour, which differ from the Markovian case. In particular, the memory can lead to large deviation principles with reduced speeds, and to non-analytic rate functions. We then explain how the mechanisms operating in these two models are generic for memory-dependent dynamics and show other examples including a non-Markovian symmetric exclusion process.

Memory effects and long-range temporal correlations are important in many physical systems [1–5], and in other scientific fields ranging from biology to telecommunications to finance [6, 7]. It is particularly notable that long-ranged memory can change fluctuation behaviour qualitatively, compared to Markovian (memory-less) cases. Demonstrations of this include non-Markovian random walks [8–12], models of cluster growth [13–15], and agent-based models where decisions depend on past experience [16]. The distinction between Markovian and non-Markovian systems is also important when formulating general theories. For example, a large deviation theory of dynamical fluctuations is now established for Markovian systems [17–22], but memory can lead to new effects which cannot be captured by the standard theory [15, 23–26]. In particular, one finds [23, 24] a breakdown of the standard large deviation principles (LDPs) that hold quite generically in finite Markovian systems [21].

In this work, we consider non-Markovian systems where the dynamics depend explicitly on a time-averaged current, whose value at time t is denoted by q_t . This is a simple type of memory that occurs in a wide range of physical models [8, 11, 15, 16, 23, 24]. Using methods of large deviation theory [17–21, 27], we show how this long-range memory can lead to anomalous fluctuations of q_t . We explain that much of this behaviour can be understood by considering two generic fluctuation mechanisms, where memory plays an intrinsic role. These general mechanisms are useful for classifying previous results for non-Markovian systems, and for identifying new phenomena.

We illustrate these mechanisms by analysing current fluctuations in the elephant random walk (ERW) of [8, 9, 28, 29], and a related process which we call the Gaussian elephant random walk (GERW). A key difference from Markovian systems is that large (rare) fluctu-

ations in these models are associated with currents that are strongly time-dependent [15, 23, 24, 27] – a large current at early times biases the subsequent evolution and can trigger anomalous fluctuations that persist for large times. The two specific mechanisms that we discuss are: (i) a very large initial current flow in a finite time interval, which results in anomalously large deviations (specifically, an LDP for q_t with a speed that is less than t [23, 24]); and (ii) a large initial current that occurs over a sustained time interval, which leads to a breakdown of the central limit theorem (CLT) for q_t [8] and an LDP which generically has a non-analytic rate function [15]. The GERW illustrates mechanism (i), which we refer to as an *initial giant leap* (IGL); the ERW illustrates mechanism (ii) which we call a *long initial excursion* (LIE). We also describe several other examples of systems in which these mechanisms occur.

Models – We consider stochastic particle systems where \mathcal{C}_t denotes the configuration at time t . Our general analysis includes complex many-particle processes, but our primary focus is on models where \mathcal{C}_t is identified with the position x_t of a single particle that moves in a finite one-dimensional domain, with discrete time steps. The displacement of the particle on step t is $\Delta x_t = \Delta \mathcal{C}_t$, and the time-averaged current is $q_t = (1/t) \sum_{\tau=1}^t \Delta \mathcal{C}_\tau$, with $q_0 = 0$. (We consider periodic boundaries so the position x_t is bounded, but q_t depends on the winding-number and is unbounded.) The systems are non-Markovian, in the sense that the displacement of the particle on step t depends on q_{t-1} , and therefore on the history of previous displacements.

In the ERW model, the configuration \mathcal{C}_t is the integer-valued position of the elephant and the dynamical rule is that $\Delta \mathcal{C}_t = \pm 1$ with probability $\frac{1}{2}(1 \pm aq_{t-1})$. Here $a \in (-1, 1)$ is a parameter that corresponds to $2p - 1$ in [8]. The GERW is similar, except that $\Delta \mathcal{C}_t$ is a Gaussian-distributed real number with mean aq_{t-1} and

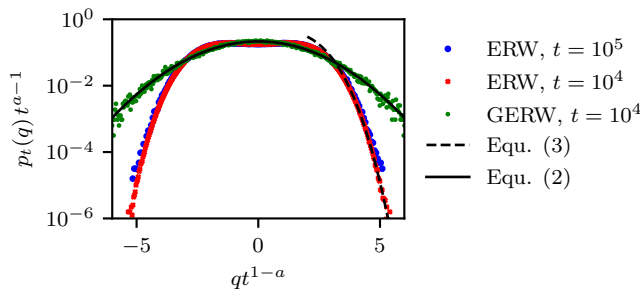


FIG. 1. Empirical distributions of the (scaled) current $t^{1-a}q_t$ for the ERW and GERW, with $a = 0.7$. The ERW data collapse when plotted as a function of this scaling variable and the tails fit well to (3). The GERW matches the exact result (2).

variance unity. For positive a the memory effect makes large fluctuations more likely. For $0 < a < \frac{1}{2}$ the memory is relatively weak, and the ERW and GERW both obey a CLT at large times, where the asymptotic variance of q_t is $1/[t(1-2a)]$. We focus here on $a > \frac{1}{2}$ where the memory effect is strong, and both models exhibit superdiffusive behaviour [8, 30]:

$$\langle q_t^2 \rangle \simeq \chi t^{-2(1-a)} \quad (1)$$

where χ is an a -dependent constant and angled brackets indicate an average over the stochastic dynamics.

Distribution of q_t – The probability density for q_t is denoted by $p_t(q)$. Simulation results in Fig. 1 show that the distributions for the ERW and GERW have quite different forms, although they both obey (1). For the GERW the distribution is Gaussian and one has for large times (see Supplemental Material (SM) [30])

$$p_t(q) \propto \exp\left[-t^{2(1-a)}q^2/(2\chi)\right]. \quad (2)$$

For the ERW, we explain below that for $t^{-(1-a)} \ll q \ll 1$ then

$$p_t(q) \propto \exp\left(-\alpha t|q|^{1/(1-a)}\right) \quad (3)$$

for some constant α (dependent on a). This behaviour is shown in Fig. 1 with a dashed line. These distributions are sharply peaked as $t \rightarrow \infty$; both systems are ergodic [10].

To explore the probability distributions and the associated fluctuation mechanisms, we use *large deviation theory* [17–21]. This theory describes rare fluctuations, outside the range of CLTs and their generalisations [9]. In recent years, it has been applied to time-averaged quantities in many physical systems, yielding important new insights [19, 31–34]. Equ. (2) is an LDP where the speed is $t^{2(1-a)}$ and the rate function is quadratic. In Markovian systems with finite state spaces, one expects very generally an LDP with speed t , that is $p_t(q) \simeq \exp[-tI(q)]$,

where I is the rate function; this is consistent with the ERW behaviour (3) but not with (2). For the GERW with $a > \frac{1}{2}$, the LDP (2) has a smaller speed than the Markovian case, which means that large fluctuations are strongly enhanced by the memory effect [23, 24], see [35–37] for some other examples where LDPs with reduced speed are associated with enhanced fluctuations. We show here that (2,3) correspond to two generic classes of non-Markovian behaviour, with two distinct fluctuation mechanisms.

Fluctuations in the GERW – Consider a discrete-time trajectory with t steps, denoted by $\mathcal{C} = (\Delta\mathcal{C}_1, \Delta\mathcal{C}_2, \dots, \Delta\mathcal{C}_t)$. It occurs with probability $P(\mathcal{C})$. In the GERW, $P(\mathcal{C})$ is a multivariate Gaussian distribution, so all correlations can be computed exactly (at fixed t). In particular, the most likely path that achieves $q_t = q$ can be derived, by conditioning $P(\mathcal{C})$ on this rare event [30]. For later comparison with the ERW, note that one can also construct an optimally-controlled process (or auxiliary process) whose typical dynamics generates the most likely path to $q_t = q$. This is similar to the Doob-transformed dynamics of [21, 38], see also [39–43]. For the GERW, we have derived the optimally-controlled process and the typical path $\langle q_\tau \rangle_{\text{con}}$ (for $\tau = 1, 2, \dots, t$) [30]. Results illustrating this path are shown in Fig. 2(a), where they are compared with the ERW. The mechanism for achieving a rare value of q_t is that the GERW makes a very large hop on the first step, after which q_τ decreases towards q_t .

For large t, τ the behaviour of this trajectory is $\langle q_\tau \rangle_{\text{con}} \approx q_t(t/\tau)^{1-a}$ [30], similar to [24]. Extrapolating this result back to $\tau = 1$ indicates that for (rare) paths that end at q_t , the first hop should have size $q_t t^{1-a}$, which diverges as $t \rightarrow \infty$. In fact the early-time behaviour is more complex [24] but the size of the first hop is indeed of this order. The diverging hop is the reason that we call this mechanism an *initial giant leap* (IGL). It applies in the Gaussian elephant for all fluctuations with $q_t = O(1)$ as $t \rightarrow \infty$.

Fluctuations in the ERW – Every jump in the ERW has size 1 so there can be no IGL. To characterise large deviations in this case, consider the scaled cumulant generating function (SCGF):

$$\psi(\lambda) = \lim_{t \rightarrow \infty} \frac{1}{t} \log \langle e^{\lambda t q_t} \rangle. \quad (4)$$

In a recent mathematical study, Franchini [27] considered large deviations in Pólya urn models, which can be mapped onto the ERW [9]. His results show that for $|\lambda| \ll 1$,

$$\psi(\lambda) \simeq |\lambda|^{1/a} c_{\text{ERW}} \quad (5)$$

for some constant c_{ERW} (dependent on a). Then (3) follows by applying a Legendre transform, leading to a large deviation rate function $I(q) = \alpha|q|^{1/(1-a)}$ for $|q| \ll 1$.

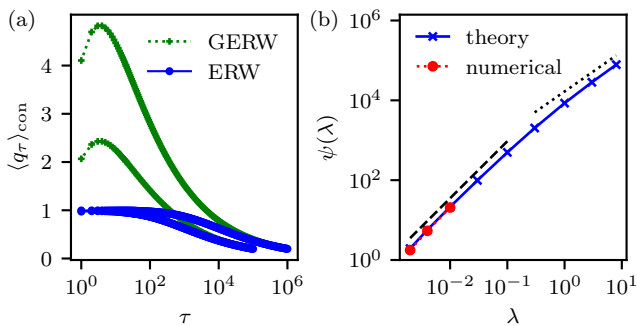


FIG. 2. (a) Averaged paths $\langle q_\tau \rangle_{\text{con}}$ of the controlled dynamics with $t = 10^5, 10^6$ and $\langle q_t \rangle_{\text{con}} = 0.2$, for the ERW and GERW with $a = 0.7$. These illustrate the IGL and LIE mechanisms. (b) Theoretical estimate for $\psi(\lambda)$ in the ERW, derived at $t = 10^4$ and compared with numerically exact results for small λ . The dashed and dotted lines indicate the predicted power laws $\psi \propto \lambda^{1/a}$ and $\psi \propto \lambda$ respectively.

Note that if q_t obeyed a CLT then its asymptotic variance would be $1/I''(0)$: here we have $I''(0) = 0$, which shows that the scaling is superdiffusive, consistent with (1).

We characterize the mechanism responsible for (5), by deriving a controlled process which captures the behaviour of the relevant conditioned path ensemble [30]. The controlled process is similar to the original process but now $\Delta \mathcal{C}_\tau = \pm 1$ with time-dependent probabilities $(1 \pm b_\tau)/2$ where (b_1, b_2, \dots, b_t) are variational parameters that we optimise, to reproduce the large-deviation mechanism [30]. This yields a controlled process with $\langle q_\tau \rangle_{\text{con}}$ as shown in Fig. 2(a): for early times, typical paths have $q_\tau \approx 1$ which is the maximum possible value in the ERW. This behaviour persists over a finite fraction of the trajectory, which motivates the name, *long excursion*. For larger times, q_τ decreases. Fig. 2(b) shows our theoretical estimate of $\psi(\lambda)$ [30], compared with numerically exact results from direct simulation. The theoretical estimate (i) matches the exact result in the region where numerical results are available; (ii) is consistent with (5) for $t^{-a} \ll \lambda \ll 1$; (iii) recovers $\psi(\lambda) \simeq |\lambda|$ for large λ , which is the exact result (since $q \leq 1$). The controlled dynamics give a good description of the true $\psi(\lambda)$, and the averaged paths shown in Fig. 2(a) also capture the fluctuation mechanism.

Fluctuation mechanisms – The IGL and LIE both rely on excursions with large current q_τ at small time, which bias all future motion towards positive current, via the memory effect. We now formulate a general theory for such excursions, which applies to continuous-time models as well as the discrete-time cases considered so far. This provides general conditions under which excursions can occur, and explains their consequences for LDPs. We consider excursions which extend over a time period between $t = 0$ and some time τ^* . Let q_∞ be the long-time

limit of $\langle q_t \rangle$. For simplicity we discuss deviations with $q_t > q_\infty$; the opposite case is a straightforward analogue. The probability $p_t(q)$ can be bounded from below by restricting to paths where the size of the excursion is at least q^* , that is $q_{\tau^*} \geq q^*$. By conditional probability:

$$\log p_t(q) \geq \log p_t(q|q_{\tau^*} \geq q^*) + \log P(q_{\tau^*} \geq q^*) \quad (6)$$

where $P(q_{\tau^*} \geq q^*)$ is the probability of the excursion and $p_t(q|q_{\tau^*} \geq q^*)$ is the corresponding conditional probability density for q_t . We write $\langle \cdot \rangle_{q^*}$ for averages that are conditioned on $q_{\tau^*} \geq q^*$. We consider excursions with $\langle q_t \rangle_{q^*} = q$ and we assume that $p_t(q|q_{\tau^*} \geq q^*)$ has a sharp peak at this value: hence (6) becomes $\log p_t(q) \gtrsim \log P(q_{\tau^*} \geq q^*)$, which is a lower bound on $p_t(q)$.

Generic IGL mechanism – The possibility of large excursions (giant leaps) leads to a quantitative bound. We first specify the probability of the excursion: assume that there is some τ^* such that $P(q_{\tau^*} \geq q^*) \simeq \exp(-\gamma|q_* - q_\infty|^\beta)$ for large q^* , with $\gamma, \beta > 0$. Also, assume that for $t \gg \tau^*$

$$\langle q_t - q_\infty \rangle_{q^*} \simeq (\tau^*/t)^{1-a} (q^* - q_\infty) \mathcal{F}(q^*, \tau^*) \quad (7)$$

for some function \mathcal{F} . Physically, this requires that after the excursion, the time-averaged current relaxes to its steady-state value as a power law with exponent $1 - a$, related to the fixed-point stability analysis of [24]. (Finite Markovian systems relax generically as t^{-1} , so a encodes the effects of memory.)

The IGL mechanism requires that (7) holds even as $q^* \rightarrow \infty$; in this limit $\mathcal{F}(q^*, \tau^*)$ should approach a finite value that we denote by f_* . Then (6,7) with $q = \langle q_t \rangle_{q^*}$ yield

$$-\log p_t(q) \lesssim t^{\beta(1-a)} |q - q_\infty|^\beta \alpha_{\text{IGL}} \quad (8)$$

where $\alpha_{\text{IGL}} = \gamma f_*^{-\beta} \tau_*^{-\beta(1-a)}$. Equ. (8) corresponds to an LDP with speed $t^{\beta(1-a)}$. If this speed is less than t , fluctuations are qualitatively larger than one finds in generic Markovian systems.

The GERW satisfies all the requirements for the IGL mechanism, with $\beta = 2$. In this case, the bound (8) is consistent with (2): it gives the right scaling with t and the correct general mechanism. However, the constant α_{IGL} obtained from this generic argument does not coincide with the prefactor in (2): obtaining that result requires a more detailed (model-dependent) calculation.

Since the bound (8) relies on simple assumptions, it is straightforward to find other models that exhibit an IGL. As an example in continuous time, we modify the unidirectional walker model of [23], which has $\Delta \mathcal{C} = 1$ for all jumps (always in the same direction). In our model the particle makes its first jump at time t_0 ; subsequent jumps occur with rate $v(q_t) = a q_t$. For $0 < a < 1$, this leads to an LDP with speed t^{1-a} , as found in [23]. The

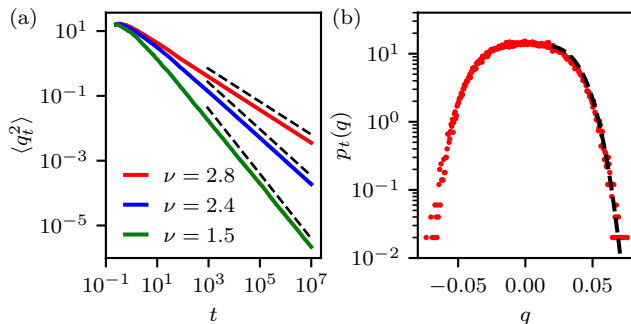


FIG. 3. Numerical results for a non-Markovian symmetric simple exclusion process with $(N, L) = (8, 16)$, so $\nu_c = 3.75$. (a) For $\nu = 2.4, 2.8$, particle motion is superdiffusive so the variance of q_t decays as a power law consistent with (1), dashed lines indicate power-law behaviour with the theoretically-predicted exponent $a = \nu/\nu_c$. For $\nu = 1.5$ the behaviour is diffusive, $\langle q_t^2 \rangle \propto t^{-1}$, since $\nu < \nu_c/2$. (b) The distribution of q_t for $\nu = 2.8$ at $t = 10^5$ is similar to the ERW in Fig. 1, the dashed black line is a fit to (3) with $a = \nu/\nu_c$.

assumptions of (6,7) above are satisfied (with $\beta = 1$) [30] so our theory shows that the mechanism for the LDP is an IGL. Note that $t_0 > 0$ is a fixed parameter in this model; this is necessary to regularise the behaviour at short times [30]. While the role of a in this analysis has some similarities to [23, 24], we emphasize that (8) is derived by considering trajectories where the excursion size q^* diverges as $t \rightarrow \infty$. The necessity of this (divergent) giant leap was neglected in [24], which means that those results apply to the GERW but fail for the ERW.

Generic LIE mechanism – The ERW behaviour is explained by the LIE mechanism, which differs from the IGL in that the excursion has finite q_* but diverging τ_* (proportional to t). We show that this general picture is consistent with an LDP with speed t : in that case the excursion has $P(q_{\tau^*} \geq q^*) \simeq e^{-\tau_* I(q^*)}$. Assume also that (7) holds asymptotically for $1 \ll \tau^* \ll t$ with $\lim_{\tau^* \rightarrow \infty} \mathcal{F}(q^*, \tau^*) = f_{\ddagger}$. Then (6,7) yield

$$-\log p_t(q) \lesssim t|q - q_\infty|^{1/(1-a)} \alpha_{\text{LIE}} \quad (9)$$

which holds for $|q - q_\infty| \ll 1$, with α_{LIE} of order unity [30]. This is consistent with the assumption of an LDP with speed t . The interesting case is $a > \frac{1}{2}$, in which the curvature of the rate function vanishes at $q = q_\infty$, corresponding to superdiffusive scaling [30].

We reiterate the difference between the IGL and LIE mechanisms: The IGL makes a giant (divergent) excursion in a finite time and leads to an LDP with reduced speed. The LIE makes a finite excursion over a long (divergent) time period, it leads to an LDP with speed t , and (generically) to a rate function that is non-analytic at q_∞ . In all examples that we have managed to construct, the IGL mechanism relies on microscopic transition rates that diverge as $q_t \rightarrow \infty$, in order to satisfy (7). This mechanism has an interesting analogy with

condensation in interacting-particle systems [44, 45]: to achieve $q_t = q$ the system must support an excess current which may be distributed over a macroscopic fraction of the time period (as in the LIE), or *condensed* into a finite time interval (the IGL). A similar phenomenon is described by the “single-big-jump” principle for sums of random variables (including certain types of correlated process) [46]; the particular history-dependence in our models, with $a > 0$, constrains the condensation to take place at the beginning of the time period.

Other LIE examples – The LIE mechanism also operates in the growth model of [13, 15], in which growing clusters contain two kinds of particle, and there is a symmetry-breaking transition between mixed and demixed clusters. We identify q_t with the composition of the cluster. In the mixed (one-phase) regime, the behaviour is qualitatively similar to the ERW, and our generic LIE arguments establish a range of parameters for which (9) applies with $a > \frac{1}{2}$, hence there should be an LDP with speed t , superdiffusive scaling, and no CLT [30]. This conclusion resolves an open question from [15], regarding the speed of the LDP in this regime, and the associated large deviation mechanism.

Finally, we consider a non-Markovian symmetric exclusion process where N particles hop on a periodic one-dimensional lattice of L sites. The time-averaged current is $q_t = (Lt)^{-1} \sum_{\text{hops}} \Delta x_\tau$ where the sum is over all particle hops, with $\Delta x_\tau = \pm 1$ according to whether the hop is to the right or the left. Large deviations of q_t have been studied extensively in the Markovian case [47, 48]. We introduce a memory of mean-field type, so that every particle hops either right (+) or left (−) with rate $w_\pm = [1 \pm \tanh(\nu q_t)]/2$, as long as the destination site is empty.

As explained in SM [30], this model has a symmetry-breaking transition at $\nu_c = L(L-1)/[N(L-N)]$, like the growth models of [13–15], whose transition rates have a similar dependence on q_t . For $\nu < \nu_c$, the assumptions required for (9) are satisfied with $a = (\nu/\nu_c)$. For $\frac{1}{2} < (\nu/\nu_c) < 1$, we therefore predict superdiffusive behaviour as in (1) with an LDP similar to (3), due to the LIE mechanism. Numerical results confirming this scenario are shown in Fig. 3. This illustrates that the generic fluctuation mechanisms described here are not limited to simple one-particle systems.

Outlook – We have presented two mechanisms by which large deviations can occur in non-Markovian processes, leading to generic bounds (8,9) on the probabilities of these rare events. To prove that these bounds give the right scaling in specific cases requires more detailed analysis, as illustrated here for the simple ERW and GERW models. (Such analyses are necessary to rule out competing mechanisms with larger probability than the IGL and LIE.) Our results indicate that the LIE mechanism operates in a non-Markovian exclusion process, and the general mechanistic insights have enabled us to

clarify and extend several other results from the literature [15, 23, 24]. This understanding is also relevant in socioeconomic decision models that can be approximated by generalized urn/elephant models [16]; by revealing fluctuation mechanisms in these systems, our analysis may be utilised to predict and control their long-term fluctuations. We look forward to future work exploiting these new insights, in order to elucidate the rich fluctuation behaviour of non-Markovian systems.

-
- [1] N. C. Keim and S. R. Nagel, Phys. Rev. Lett. **107**, 010603 (2011).
- [2] C. Scalliet and L. Berthier, Phys. Rev. Lett. **122**, 255502 (2019).
- [3] J. Kappler, J. O. Daldrop, F. N. Brünig, M. D. Boehle, and R. R. Netz, J. Chem. Phys. **148**, 014903 (2018).
- [4] P. Van Mieghem and R. van de Bovenkamp, Phys. Rev. Lett. **110**, 108701 (2013).
- [5] J. Zhang and T. Zhou, Proc. Natl. Acad. Sci. USA **116**, 23542 (2019).
- [6] G. Rangarajan and M. Ding, eds., *Processes with Long-Range Correlations: Theory and Applications*, Lecture Notes in Physics, Vol. 621 (Springer-Verlag, Berlin Heidelberg, 2003).
- [7] J. Beran, Y. Feng, S. Ghosh, and R. Kulik, *Long-Memory Processes: Probabilistic Properties and Statistical Methods*, Berlin Heidelberg ed. (Springer-Verlag, 2013).
- [8] G. M. Schütz and S. Trimper, Phys. Rev. E **70**, 045101 (2004).
- [9] E. Baur and J. Bertoin, Phys. Rev. E **94**, 052134 (2016).
- [10] A. A. Budini, Phys. Rev. E **94**, 022108 (2016).
- [11] A. A. Budini, Phys. Rev. E **95**, 052110 (2017).
- [12] A. Rebenshtok and E. Barkai, Phys. Rev. Lett. **99**, 210601 (2007).
- [13] K. Klymko, J. P. Garrahan, and S. Whitelam, Phys. Rev. E **96**, 042126 (2017).
- [14] K. Klymko, P. L. Geissler, J. P. Garrahan, and S. Whitelam, Phys. Rev. E **97**, 032123 (2018).
- [15] R. L. Jack, Phys. Rev. E **100**, 012140 (2019).
- [16] R. J. Harris, New J. Phys. **17**, 053049 (2015).
- [17] F. den Hollander, *Large deviations* (American Mathematical Society, Providence, RI, 2000).
- [18] V. Lecomte, C. Appert-Rolland, and F. van Wijland, J. Stat. Phys. **127**, 51 (2007).
- [19] B. Derrida, J. Stat. Mech. **2007**, P07023 (2007).
- [20] H. Touchette, Phys. Rep. **478**, 1 (2009).
- [21] R. Chétrite and H. Touchette, Ann. Henri Poincaré **16**, 2005 (2015).
- [22] R. L. Jack, arXiv:1910.09883 (2019).
- [23] R. J. Harris and H. Touchette, J. Phys. A **42**, 342001 (2009).
- [24] R. J. Harris, J. Stat. Mech. **2015**, P07021 (2015).
- [25] C. Maes, K. Netočný, and B. Wynants, J. Phys. A **42**, 365002 (2009).
- [26] A. Faggionato, arXiv:1709.05653 (2017).
- [27] S. Franchini, Stoch. Process. Appl. **127**, 3372 (2017).
- [28] B. Bercu, J. Phys. A **51**, 015201 (2017).
- [29] V. M. Kenkre, arXiv:0708.0034.
- [30] Supplemental Material, including Ref. [49].
- [31] J. Lebowitz and H. Spohn, J. Stat. Phys. **95**, 333 (1999).
- [32] J. P. Garrahan, R. L. Jack, V. Lecomte, E. Pitard, K. van Duijvendijk, and F. van Wijland, Phys. Rev. Lett. **98**, 195702 (2007).
- [33] L. O. Hedges, R. L. Jack, J. P. Garrahan, and D. Chandler, Science **323**, 1309 (2009).
- [34] T. R. Gingrich, J. M. Horowitz, N. Perunov, and J. L. England, Phys. Rev. Lett. **116**, 120601 (2016).
- [35] D. Nickelsen and H. Touchette, Phys. Rev. Lett. **121**, 090602 (2018).
- [36] G. Gradenigo and S. N. Majumdar, J. Stat. Mech. **2019**, 053206 (2019).
- [37] B. Meerson, Phys. Rev. E **100**, 042135 (2019).
- [38] R. Chétrite and H. Touchette, J. Stat. Mech. **2015**, P12001 (2015).
- [39] C. Maes and K. Netočný, EPL **82**, 30003 (2008).
- [40] A. Simha, R. M. L. Evans, and A. Baule, Phys. Rev. E **77**, 031117 (2008).
- [41] D. Simon, J. Stat. Mech. **2009**, P07017 (2009).
- [42] R. L. Jack and P. Sollich, Prog. Theor. Phys. Supp. **184**, 304 (2010).
- [43] R. L. Jack and P. Sollich, Eur. Phys. J.: Spec. Topics **224**, 2351 (2015).
- [44] S. Grosskinsky, G. M. Schütz, and H. Spohn, J. Stat. Phys. **113**, 389 (2003).
- [45] M. R. Evans and B. Waclaw, J. Phys. A: Math. Theor. **47**, 095001 (2014).
- [46] A. Vezzani, E. Barkai, and R. Burioni, Phys. Rev. E **100**, 012108 (2019).
- [47] C. Appert-Rolland, B. Derrida, V. Lecomte, and F. van Wijland, Phys. Rev. E **78**, 021122 (2008).
- [48] V. Lecomte, J. P. Garrahan, and F. van Wijland, J. Phys. A **45**, 175001 (2012).
- [49] P. Dupuis and R. S. Ellis, *A weak convergence approach to the theory of large deviations* (Wiley, 1997).

SUPPLEMENTAL MATERIAL

Optimal control theory

We provide here some additional derivations and numerical results, to support the results of the main text.

Typical fluctuations in the GERW and ERW

In this section we derive (1) for the GERW. Suppose that after t steps $Q_t = tq_t$ has a Gaussian distribution with mean zero and variance v_t . Then $Q_{t+1} - Q_t$ is normally distributed with mean aq_t and variance 1 so the distribution of Q_{t+1} is

$$p(Q_{t+1}) = \frac{1}{\sqrt{4\pi^2 v_t}} \int e^{-[Q_{t+1} - Q_t(1 + \frac{a}{t})]^2 / 2 - Q_t^2 / (2v_t)} dQ_t \quad (10)$$

which is normal with mean zero and variance $v_{t+1} = 1 + v_t(1 + a/t)^2$. This recursion gives a series solution for v_t ; here we derive the long-time behaviour. For large t we write $v_t = v(t)$ and find $v'(t) \approx 1 + 2av(t)/t$. Hence $v(t) \approx t/(1 - 2a) + ct^{2a}$ and so the variance of q_t is $v(t)/t^2 \approx 1/[t(1 - 2a)] + ct^{-2(1-a)}$ with the second term dominant for $a > \frac{1}{2}$.

The results in Fig. 1 of the main text are obtained by direct simulation. The Gaussian fit to the GERW data corresponds to $\chi = 3.4$ in (2) which was estimated by computing numerically the variance for the first 40 hops using the recursion formula for v_t given above.

For comparison with the ERW, beyond the level of the first and second moments, we also analyse the cumulant generating function (CGF) which has

$$G(\lambda, t) = \log \langle e^{\lambda tq_t} \rangle. \quad (11)$$

For large t in the GERW one has from (2) that

$$G(\lambda, t) \simeq \frac{\lambda^2 t^{2a} \chi}{2}. \quad (12)$$

This is quadratic in λ , as expected because the distribution of Q_t is Gaussian at all times.

We now turn to the ERW. Since the derivatives of G give cumulants of Q_t , one has $G(\lambda, t) = \lambda^2 \text{Var}(Q_t)/2 + O(\lambda^3)$. The variance of Q_t satisfies a similar recursion to the GERW [8], which again yields (1). For $t \gg 1$ and very small λ , it follows that both the ERW and the GERW follow (12), with different constants χ .

However, the ERW does not have a Gaussian distribution for Q_t , and $G(\lambda, t)$ only coincides with (12) for very small $\lambda \ll t^{-a}$ (with $t^{-a} \ll 1$ because t is large). In fact, for $t^{-a} \ll \lambda \ll 1$ then the analytical result (5) requires that $G(\lambda, t) \sim |\lambda|^{1/a}$. Moreover, the scaling collapse shown in Fig. 1 indicates that G should be a scaling function of λt^a , which is consistent with (1). Fig. 4 verifies the consistency of this picture: (i) for small λt^a the CGF for the ERW is proportional to $|\lambda t^a|^2$ and matches the large- t GERW result; (ii) for larger λt^a then the CGF for the ERW is proportional to $|\lambda t^a|^{1/a}$.

As discussed in the main text, we analyse fluctuation mechanisms by constructing controlled processes whose typical trajectories reproduce the rare-event behaviour of the ERW and GERW. Such processes can be analysed variationally, as follows. The probability of path \mathcal{C} in the original model is $P(\mathcal{C})$. Throughout our analysis, we fix t as the trajectory length and we use τ to indicate a generic time within the trajectory. Now let $P_{\text{con}}(\mathcal{C})$ be the probability of \mathcal{C} in some controlled model, which has different dynamics. Optimal-control theory provides the following general inequality [49]

$$G(\lambda, t) \geq \lambda t \langle q_t \rangle_{\text{con}} - \mathcal{D}(P_{\text{con}} || P) \quad (13)$$

where $\langle \cdot \rangle_{\text{con}}$ indicates an average in the controlled model, and $\mathcal{D}(Q || P)$ is the Kullback-Leibler (KL) divergence between the distributions Q and P . To prove (13) define

$$P_{\text{cano}}(\mathcal{C}) = e^{\lambda tq_t - G(\lambda, t)} P(\mathcal{C}) \quad (14)$$

which is a normalised probability distribution, by definition of G . (The subscript ‘‘cano’’ indicates that this definition is analogous to that of the canonical ensemble in thermodynamics.) Then by definition of the KL divergence, the right-hand side of (13) can be expressed as

$$\lambda t \langle q_t \rangle_{\text{con}} - \mathcal{D}(P_{\text{con}} || P) = G(\lambda, t) - \mathcal{D}(P_{\text{con}} || P_{\text{cano}}). \quad (15)$$

The KL divergence is non-negative so this is less than or equal to $G(\lambda, t)$ and (13) follows. Moreover, there is equality in (13) if and only if $P_{\text{con}} = P_{\text{cano}}$.

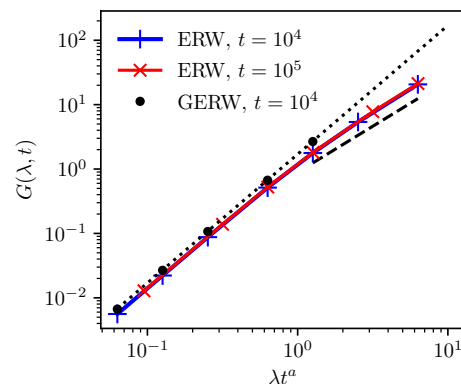


FIG. 4. CGFs for the ERW and GERW, plotted as a function of the scaling variable λt^a . We take $a = 0.7$ as in Fig. 1. The dotted line shows the analytical (large- t) GERW result $G(\lambda, t) = \chi(\lambda t^a)^2/2$, which is consistent with the numerical data. The ERW data do not follow a simple power law but show a scaling collapse to a non-trivial function $f(\lambda t^a)$, consistent with the behaviour shown in Fig. 1; the numerics match the GERW for $\lambda \lesssim t^{-a}$ before crossing over to $G(\lambda, t) \simeq c_{\text{ERW}} |\lambda t^a|^{1/a}$ for $\lambda \gtrsim t^{-a}$ (with the latter power-law behaviour indicated by a dashed line of gradient $1/a$).

In addition, by definition (4), we have that $\psi(\lambda) = \lim_{t \rightarrow \infty} t^{-1} G(\lambda, t)$ so (13) yields

$$\psi(\lambda) \geq \lim_{t \rightarrow \infty} \left[\lambda \langle q_t \rangle_{\text{con}} - \frac{1}{t} \mathcal{D}(P_{\text{con}} \| P_{\text{cano}}) \right]. \quad (16)$$

If this bound is saturated then the controlled process gives an accurate representation of the rare event of interest, see also below. We emphasise that for non-Markovian processes as considered here, the limit in (16) involves controlled processes where the dynamical rule at time τ depends both on τ and on the total trajectory length t ; accurate bounds require controlled processes with time-dependent rates.

Large deviations in the GERW

We derive the most likely path associated with large deviations of q_t in the GERW, as plotted in Fig. 2. The path probability distribution $P(\mathcal{C})$ may be constructed as a function of the q_τ , as $P(\mathcal{C}) \propto \exp(-\mathcal{S}/2)$ with

$$\mathcal{S} = \sum_{\tau=0}^{t-1} [(\tau+1)q_{\tau+1} - q_\tau(\tau+a)]^2 \quad (17)$$

where $q_0 = 0$. Collecting terms, one obtains

$$\begin{aligned} \mathcal{S} = t^2 q_t^2 + \sum_{\tau=1}^{t-1} q_\tau^2 (2\tau^2 + a^2 + 2a\tau) \\ - 2 \sum_{\tau=1}^{t-1} q_\tau q_{\tau+1} (\tau+1) (\tau+a). \end{aligned} \quad (18)$$

Conditioning on q_t , we arrive at a Gaussian distribution for the $(t-1)$ -dimensional vector $\mathbf{q} = (q_1, q_2, \dots, q_{t-1})$. This is $P_{\text{micro}}(\mathbf{q}|q_t) = \exp(hq_t q_{t-1} - \mathbf{q}^T M \mathbf{q}/2)/C(q_t)$, where $h = t(t+a-1)$. Here $C(q_t)$ is a normalisation constant and M is a matrix whose elements can be read from (18). The subscript ‘‘micro’’ recalls that conditioning $q_t = q$ is analogous to considering a microcanonical ensemble in thermodynamics. Completing the square in the exponent, one obtains

$$P_{\text{micro}}(\mathbf{q}|q_t) \propto \exp[-(\mathbf{q} - hq_t \boldsymbol{\mu})^T M (\mathbf{q} - hq_t \boldsymbol{\mu})/2] \quad (19)$$

where $\boldsymbol{\mu}$ is given by the $(t-1)$ th column of M^{-1} and, for brevity, we do not explicitly write the normalisation constant. Hence the most likely path with $q_t = q$ is given by

$$\langle q_\tau \rangle_{\text{micro}} = \mu_\tau q h. \quad (20)$$

For finite t , this can be straightforwardly computed numerically.

However, we are interested in long paths (for example, $t \gtrsim 10^4$), so a simplifying approximation is useful. We

characterise the most likely path as the minimum of the exponent in (19). Writing the matrix product as a sum over time steps, we fix some K and separate the sum into terms with $\tau \leq K$ and $\tau > K$. For $\tau > K$ we replace $q_\tau \rightarrow \tilde{q}(\tau)$ where \tilde{q} is a smooth function of τ ; this allows the sum to be estimated by an integral. Fixing values for q_K, q_t , the action can be minimised (exactly) over the function \tilde{q} , which is equivalent to solving the instanton equation in [24]. One finds $\tilde{q}(\tau) = C_1 \tau^{-a} + C_2 \tau^{-(1-a)}$ where C_1, C_2 are fixed by the boundary conditions at $\tau = K, t$. The contribution to \mathcal{S} from this path is [24]

$$\mathcal{S}_1 = K(2a-1) \frac{(1 - (K/t)^{2a-1}) [q_t - q_K (K/t)^{1-a}]^2}{[(K/t)^a - (K/t)^{1-a}]^2}. \quad (21)$$

Hence (17) reduces (for this optimal path) to

$$\mathcal{S} = \sum_{\tau=0}^{K-1} [(\tau+1)q_{\tau+1} - q_\tau(\tau+a)]^2 + \mathcal{S}_1 \quad (22)$$

which is to be minimised over q_1, q_2, \dots, q_K . This yields the GERW paths in Fig. 2(a). We typically take $K = 40$, this choice does not strongly affect the results because replacing the discrete sum by an integral is accurate for $K \gg 1$.

Since the path probability distribution is Gaussian in this system, one may also construct the optimally-controlled process that achieves equality in (16). Using (14) one obtains a distribution for the full path $\mathcal{C} = (\mathbf{q}, q_t)$:

$$P_{\text{cano}}(\mathcal{C}) \propto e^{\lambda t q_t - G(\lambda, t) - (\mathcal{S}/2)}. \quad (23)$$

This distribution is still Gaussian, and one has an analogue of (20) which is

$$\langle q_\tau \rangle_{\text{cano}} = \mu_\tau \langle q_t \rangle_{\text{cano}} h \quad (24)$$

where h, μ_τ are the same quantities that appear in (20). That is, choosing λ in the canonical ensemble fixes $\langle q_t \rangle_{\text{cano}}$. Then the average path in this ensemble coincides with the average path in a corresponding microcanonical ensemble with $q_t = \langle q_t \rangle_{\text{cano}}$.

Since P_{cano} in (23) is Gaussian, it is possible to construct exactly an optimally-controlled process that generates trajectories according to P_{cano} . This process achieves equality in (13) and captures the mechanism by which large rare fluctuations occur in the GERW. This is similar to the Doob transform, as discussed in [21], with time-dependent rates as in [15]. Within the controlled system, the displacement on step τ is Gaussian with mean $aq_{\tau-1} + b_\tau$ and variance unity. This means that $P_{\text{con}}(\mathcal{C}) = \exp(-\tilde{\mathcal{S}}/2)$ with

$$\tilde{\mathcal{S}} = \sum_{\tau=0}^{t-1} [(\tau+1)q_{\tau+1} - q_\tau(\tau+a) - b_{\tau+1}]^2 \quad (25)$$

analogous to (17). Hence

$$\tilde{\mathcal{S}} = \mathcal{S} - 2tq_t b_t + 2 \sum_{\tau=1}^{t-1} q_\tau [(\tau+a)b_{\tau+1} - \tau b_\tau] + \sum_{\tau=1}^t b_\tau^2. \quad (26)$$

The optimally-controlled process has $P_{\text{con}} = P_{\text{cano}}$ [recall (15)], which is achieved by setting $b_t = -\lambda$ and using $b_{\tau-1} = b_\tau(1 + \frac{a}{\tau-1})$ iteratively to fix the b_τ . For the CGF this identification yields $G(\lambda, t) = \frac{1}{2} \sum_{\tau=1}^t b_\tau^2$.

Large deviations in the ERW

For the ERW, a variational characterisation of $\psi(\lambda)$ in (4) is available following [27]. This construction also allows computation of the dominant paths shown in Fig. 2.

We outline the approach, which is to define a controlled process that *almost* achieves equality in (13), up to a correction that vanishes on taking the limit in (16). The typical path of this controlled model captures the mechanism of the (rare) fluctuations that achieve $q_t = q$ in the ERW. (Specifically, for large t and any $u > 0$, the conditional distribution of q_{ut} for paths that achieve $q_t = q$ is sharply peaked at $\langle q_{ut} \rangle_{\text{con}}$, see [27].)

We use (13) with the controlled dynamics described in the main text for which (b_1, b_2, \dots, b_t) are variational parameters. The KL divergence between P_{con} and P is

$$\begin{aligned} \mathcal{D} = & \frac{1}{2} \sum_{\tau=1}^t [(1+b_\tau) \log(1+b_\tau) + (1-b_\tau) \log(1-b_\tau)] \\ & - \frac{1}{2} \sum_{\tau=1}^t (1+b_\tau) \langle \log(1+aq_{\tau-1}) \rangle_{\text{con}} \\ & - \frac{1}{2} \sum_{\tau=1}^t (1-b_\tau) \langle \log(1-aq_{\tau-1}) \rangle_{\text{con}}, \quad (27) \end{aligned}$$

and we have

$$\langle q_\tau \rangle_{\text{con}} = \frac{1}{\tau} \sum_{k=1}^{\tau} b_k. \quad (28)$$

Moreover, the variance of q_τ in this controlled process is at most $1/\tau$ so it is consistent to assume that q_τ is sharply peaked for almost all terms in the sums in (27). Hence $\mathcal{D} \approx \hat{\mathcal{D}}$ with

$$\begin{aligned} \hat{\mathcal{D}} = & \frac{1}{2} \sum_{\tau} [(1+b_\tau) \log(1+b_\tau) + (1-b_\tau) \log(1-b_\tau)] \\ & - \frac{1}{2} \sum_{\tau} (1+b_\tau) \log(1 + \langle aq_{\tau-1} \rangle_{\text{con}}) \\ & - \frac{1}{2} \sum_{\tau} (1-b_\tau) \log(1 - \langle aq_{\tau-1} \rangle_{\text{con}}). \quad (29) \end{aligned}$$

Using (28) this is an explicit function of the b_τ variables, so the right-hand side of (13) can be maximised numerically, which yields a numerical estimate of $G(\lambda, t)$ and

hence (by considering large but finite t) one may estimate $\psi(\lambda)$.

For numerical work we use a similar method to that for the GERW: we split the sums in (29) into contributions from small τ and large τ and we approximate the sum over large- τ contributions by an integral. This combination of sum and integral is maximised numerically to obtain estimates of $\psi(\lambda)$ and of the corresponding (average) path (28). This yields the results of Fig. 2.

IGL mechanism in unidirectional hopping model

We now establish a bound, based on the IGL mechanism, for the probability of large deviations in the unidirectional model of the main text. The model is based on a system defined in [23], the results of which indicate that large deviations with $q_t > 0$ involve a giant leap of size $q^* \sim t^{1-a}$, leading to an LDP with speed t^{1-a} . However, that work made an assumption of temporal additivity which (strictly-speaking) is valid only for $t_0 \gg 1$. Here we discuss the case where t_0 takes any positive value; we show that the IGL mechanism operates, and $p_t(q)$ can be bounded as in (8), which is consistent with an LDP with speed t^{1-a} .

To this end, consider a controlled process where the first hop is at time t_0 (as for the original model), after which hops take place with a time-dependent rate $b(\tau)$. Then $(\tau q_\tau - 1)$ is Poissonian with mean $\int_{t_0}^{\tau} b(k) dk$ and so

$$\tau \langle q_\tau \rangle_{\text{con}} = 1 + \int_{t_0}^{\tau} b(k) dk. \quad (30)$$

Considering trajectories on the time interval $[0, \tau]$, the KL divergence of (13) is

$$\mathcal{D} = \int_{t_0}^{\tau} \left\{ b(k) \left\langle \log \frac{b(k)}{aq_k} \right\rangle_{\text{con}} - b(k) + \langle aq_k \rangle_{\text{con}} \right\} dk, \quad (31)$$

similar to (27). In addition to (13), the KL divergence also allows a bound on the probability distribution of q_t . Roughly speaking, if one can construct a controlled process such that $P_{\text{con}}(q_\tau \geq q) = 1$ then the probability of this event in the original model can be bounded from below:

$$-\log P(q_\tau \geq q) \leq \mathcal{D}(P_{\text{con}} || P). \quad (32)$$

This may be proved by Jensen's inequality; a more precise statement is given (for example) in Eqs. (14,15) of [15]. Hence we seek an upper bound on \mathcal{D} .

To achieve this, we use $\log(1/x) \leq (1/x) - 1$ with $x =$

$q_k/\langle q_k \rangle_{\text{con}}$ to write

$$\mathcal{D} \leq \int_{t_0}^{\tau} \left\{ b(k) \log \frac{b(k)}{a \langle q_k \rangle_{\text{con}}} - 2b(k) + \langle a q_k \rangle_{\text{con}} + b(k) \langle q_k \rangle_{\text{con}} \left\langle \frac{1}{q_k} \right\rangle_{\text{con}} \right\} dk. \quad (33)$$

For a Poisson random variable X with mean \bar{x} , one has $\langle \frac{1}{1+X} \rangle = e^{-\bar{x}} \sum_{n=0}^{\infty} \bar{x}^n / (n+1)! = (1 - e^{-\bar{x}}) / \bar{x}$. Since $\langle k q_k - 1 \rangle$ is Poissonian, we obtain

$$\mathcal{D} \leq \int_{t_0}^{\tau} \left\{ b(k) \log \frac{b(k)}{\langle a q_k \rangle_{\text{con}}} - 2b(k) + \langle a q_k \rangle_{\text{con}} + b(k) \langle k q_k \rangle_{\text{con}} \frac{1 - e^{-\langle k q_k - 1 \rangle_{\text{con}}}}{\langle k q_k - 1 \rangle_{\text{con}}} \right\} dk. \quad (34)$$

To recover the results of [24] one should assume that $k q_k \gg 1$ throughout the integration range, so that the second line of this expression reduces to $b(k)$. This is valid for $t_0 \gg 1$. Then one sets $\tau = t$ and minimises the resulting KL divergence over the path $\hat{q}(k) = \langle q_k \rangle_{\text{con}}$, using (30) to replace $b(k) \rightarrow (\partial/\partial k)(k \hat{q}(k))$. The optimal path behaves for short times as $k \hat{q}(k) = 1 + A(k - t_0)$ where A is proportional to the size of the giant excursion [24].

Our approach here does not require t_0 to be large: we retain all terms in (34), and use (32) with $\tau = \tau^*$ to bound the probability of the excursion that appears in (6) of the main text. To obtain a convenient bound we set $\tau^* = 2t_0$ and choose $b(k)$ such that $\langle k q_k \rangle_{\text{con}} = 1 + Ax$ with $x = (k - t_0)/t_0$ and $A = 2q^* t_0 - 1$. This requires $b(k) = A/t_0$ and ensures that $\langle q_{\tau^*} \rangle_{\text{con}} = q^*$. (Note, $b(k)$ is only independent of k during the excursion ($t < \tau^*$), the controlled process reverts to the natural dynamics of the model for $t > \tau^*$.) Then (34) with $\tau = \tau^*$ becomes

$$\mathcal{D} \leq A \int_0^1 \left\{ \log \frac{A(1+x)}{a(Ax+1)} - 2 + \frac{a(Ax+1)}{A(1+x)} + (1+Ax) \frac{1 - e^{-Ax}}{Ax} \right\} dx. \quad (35)$$

We are concerned with the limit $q^* \rightarrow \infty$ which corresponds to $A \rightarrow \infty$. It can be verified that the integral is finite in this limit so the KL divergence scales as

$$\mathcal{D} \lesssim \gamma_{\text{uni}} q^* t_0 \quad (36)$$

with γ_{uni} finite as $q^* \rightarrow \infty$. Using additionally that the distribution of q_{τ^*} is sharply-peaked in this limit, (32) is applicable and the probability of the excursion obeys

$$\log P(q_{\tau^*} \geq q^*) \gtrsim -\gamma_{\text{uni}} q^* t_0 \quad (37)$$

for large q^* . This is the first condition required for the IGL mechanism, that $P(q_{\tau^*} \geq q^*) \gtrsim e^{-\gamma|q - q_{\infty}|^{\beta}}$: here

$\beta = 1$ and $q_{\infty} = 0$ and $\gamma = \gamma_{\text{uni}} t_0$. Physically, the probability of a large excursion scales exponentially in its size.

After the excursion we have the exact formula

$$\tau(\partial/\partial\tau)\langle q_{\tau} \rangle_{q^*} = (a-1)\langle q_{\tau} \rangle_{q^*}, \quad (38)$$

which comes from the dynamics of the original unidirectional model. Integrating this equation yields $(q_{\tau}/q^*) = (\tau_*/\tau)^{1-a}$ which is (7) with $q_{\infty} = 0$ and $\mathcal{F}(q^*, \tau^*) = 1$, note that this holds even as $q^* \rightarrow \infty$, which is related to the fact that $v(q^*)$ diverges in this limit. Hence all the ingredients are in place to obtain the bound (8) with $\beta = 1$ and $f_* = 1$, that is

$$-\log p_t(q) \lesssim 2^{a-1} \gamma_{\text{uni}} q t_0^a t^{1-a}, \quad (39)$$

where we used $\tau^* = 2t_0$, from above. This is the main result of this calculation: it indicates that the system has an LDP with speed t^{1-a} . A similar result was derived in [23], assuming temporal additivity. Our analysis avoids this assumption; it also shows that the unusual speed of the LDP arises because the fluctuation mechanism is an IGL.

This analysis also shows that the assumption $t_0 > 0$ is necessary: as $t_0 \rightarrow 0$ one might infer from (39) that $p_t(q) = O(1)$. In fact this interpretation is too simplistic: subleading terms were neglected in (36), and it is also not safe to assume that the distribution of q_{τ^*} is sharply-peaked in cases where $q^* t_0$ is not large. A detailed investigation of the case $t_0 = 0$ is beyond the scope of this work but preliminary results indicate that the fluctuations of q_t are large and there may be no LDP.

Note that we have considered here the unidirectional model with $v(q) = aq$, but the main ingredient required in this analysis is in fact $\lim_{q \rightarrow \infty} [v(q)/q] = a$ (with $0 < a < 1$). We expect the IGL mechanism to operate for a broad class of models where this assumption holds.

Large deviations from generic LIE

To derive (9), note that the condition (7) applies for $1 \ll \tau^* \ll t$ which means that $\langle q_t - q_{\infty} \rangle \ll 1$. Then (9) follows from (6), assuming as usual that $\log p_t(q|q_{\tau^*} \geq q^*)$ is negligible compared to $\log P(q_{\tau^*} \geq q^*) = -\tau^* I(q^*)$, which is large and negative. One finds

$$\alpha_{\text{LIE}} = I(q^*) \left(\frac{1}{|q^* - q_{\infty}| f_{\ddagger}} \right)^{1/(1-a)}. \quad (40)$$

with $f_{\ddagger} = \lim_{\tau^* \rightarrow \infty} \mathcal{F}(q^*, \tau^*)$. (This should be compared with the quantity $f_* = \lim_{q^* \rightarrow \infty} \mathcal{F}(q^*, \tau^*)$ that is relevant for the IGL mechanism.)

From (9) one obtains a bound on the scaled cumulant generating function, as

$$\psi(\lambda) \geq \sup_q [\lambda q - |q - q_{\infty}|^{1/(1-a)} \alpha_{\text{LIE}}] \quad (41)$$

which gives

$$\psi(\lambda) \geq \lambda q_\infty + |\lambda|^{1/a} c_{\text{LIE}} \quad (42)$$

with

$$c_{\text{LIE}} = a \left(\frac{1-a}{\alpha_{\text{LIE}}} \right)^{(1/a)-1}. \quad (43)$$

LIE in cluster growth models

The cluster growth models of [13,14,15] can be expressed in the general framework of this paper. One works in discrete time and identifies q_t with the magnetisation of the growing cluster, which was m_k in [15]. Considering the irreversible model of [14], the dynamical update is $\Delta \mathcal{C}_t = \pm 1$ with probabilities $(1 \pm \tanh Jq_{t-1})/2$, similar to the ERW but now with a non-linear dependence on q_{t-1} . As a controlled process we take $\Delta \mathcal{C}_t = \pm 1$ with probabilities $(1 \pm b_t)/2$, as considered here for the ERW. The KL divergence for this case is given in [15]. We focus here on the one-phase regime which is $J < 1$, for which $q_\infty = 0$ and (7) holds for small $\langle q_t \rangle_{\text{con}}$, with $a = J$.

In this situation all requirements are in place for the LIE mechanism. For $J > \frac{1}{2}$ this implies superdiffusive scaling as in (1), which was discussed in [15]. The results presented here extend that work and clarify the situation for large deviations, with the regime $\frac{1}{2} < J < 1$ again of particular interest. Specifically, it is clear from the dynamical rule that $q_* \leq 1$ so the IGL mechanism is not possible, but the LIE mechanism does occur. The result is an LDP with speed t , whose rate function is generically singular at $q = 0$, similar to (3). This scenario was discussed in [15], where the possibility of an LDP with speed less than t was also considered. The analysis of the present work shows that the IGL is not possible and one therefore expects the LIE mechanism to apply, leading to an LDP with speed t . This is consistent with the theory of [27].

Non-Markovian SSEP

The non-Markovian SSEP is defined in the main text, its dynamical rules have some similarities with the cluster growth model described above. It is useful to note that whatever the value of q_t , the dynamical rules are balanced with respect to a state where the N particles are distributed independently at random across the L sites, subject to the exclusion constraint (at most one particle per site). To be precise, detailed balance is broken (except for $q_t = 0$), but the dynamical rules for any given q_t correspond to an asymmetric simple exclusion process with periodic boundaries, whose stationary state has all particles distributed independently. Hence if the time-averaged current at time t is q_t then the (average) rate for accepted particle hops is

$$\frac{\partial}{\partial t} \langle Ltq_t \rangle = N \frac{L-N}{L-1} \tanh(\nu q_t); \quad (44)$$

this average is conditioned on the value of q_t , the factor of $(L-N)/(L-1)$ is the probability that a site adjacent to a given particle is vacant. Expanding the tanh about $q_t = 0$ shows that the zero-current state $\langle q_t \rangle = 0$ is stable only if $\nu < \nu_c$ with $\nu_c = L(L-1)/[N(L-N)]$. We identify ν_c as a critical point, directly analogous to the cluster-growth model.

For $\nu < \nu_c$, the expansion of (44) about $q_t = 0$ yields (7) with $a = \nu/\nu_c$, which is again similar to the growth model and indicates that the LIE scenario is applicable. As a controlled model we here consider a (Markovian) asymmetric simple exclusion process with a time-dependent asymmetry parameter, so hops in the (\pm) -direction have $w_\pm = (1 \pm b_t)/2$. In this case the KL divergence may be computed similarly to (27). This allows optimisation of a controlled dynamics that obeys an LIE mechanism. However, this controlled model is unlikely to be sufficient to capture the true optimal control since it neglects interparticle correlations which are important for large deviations in exclusion processes [47]. This effect might be captured by combining the temporal additivity principle [24] with results for large deviations in Markovian exclusion processes [47], but such an analysis is beyond the scope of the present work.